UPPSALA
UNIVERSITET

Impact of the chemokine receptor CX3CR1 on macrophage-nerve interactions in the pancreas

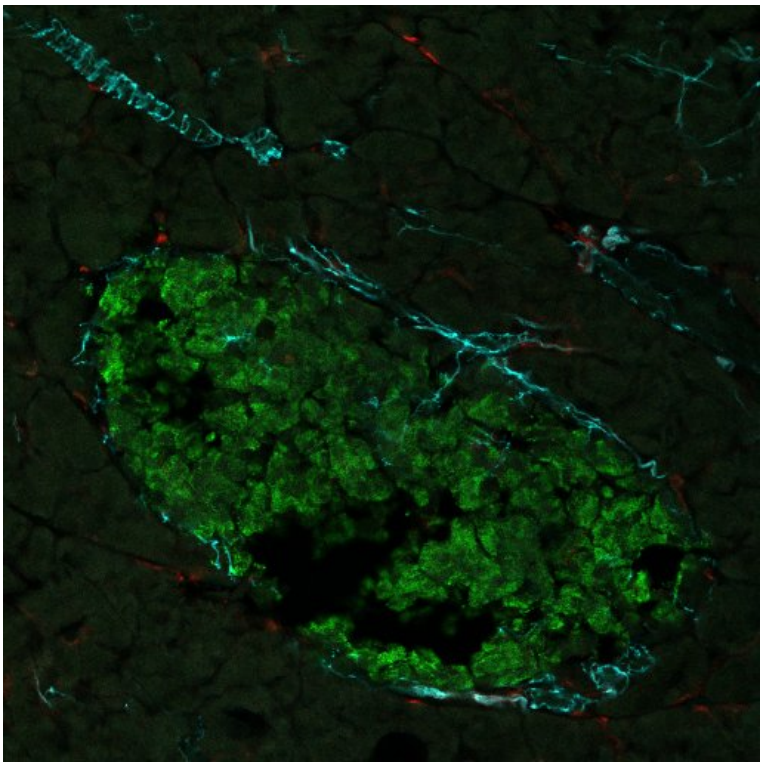

Marleen Bootsma

Degree project in biology, Master of science (2 years), 2024
Examensarbete i biologi 60 hp till masterexamen, 2024
Biology Education Centre and Department of Medical Cell Biology, Uppsala University
Supervisors: Gustaf Christoffersson and Elke Muntjewerff
External opponent: Maria Ovezik

Abstract

Diabetes type 1 (T1D) is an autoimmune disease which is characterized by an absence of insulin producing cells. There is currently no cure for T1D, and treatment involves managing symptoms through insulin therapy and other medications. T1D is believed to result from a combination of genetic predisposition and environmental triggers. While certain genes can increase the risk of developing T1D, environmental factors, such as viral infections, may trigger the autoimmune response. T1D is not caused by diet or lifestyle, though these factors can influence disease management and overall health.

This study aimed to investigate how macrophages and nerves communicate through the CX_3CR1-CX_3CL1 receptor/ligand axis. This was achieved by visualizing and quantifying the colocalization of nerves and macrophages in the kidneys, lungs, and heart of wildtype and CX_3CR1 knockout (CKO) mice, and by studying macrophage responses to nerve signals *in vitro.* CKO mice were used because nerve-associated macrophages (NAMs) highly express CX_3CR1, the receptor for fractalkine (CX_3CL1). Fractalkine is known to attract T cells and monocytes to sites of inflammation and may play a crucial role in nerve-macrophage interactions. Investigating this axis is particularly relevant to T1D, a disease characterized by T cell-mediated islet destruction. We found CX_3CR1 to be important for nerve-macrophage interactions in the kidneys and lungs but not the heart.

To understand the role of the neuropeptide catestatin on nerve-macrophage communication in the pancreas, we conducted a similar experiment as described above. This part of the study utilized microscopy imaging data from the pancreas of catestatin (CST)-knockout (KO), chromogranin A (CgA)-KO, and wild-type (WT) mice. The pancreas of CgA-KO had a higher nerve ratio per islet compared to WT and CST-KO suggesting an absence of CgA promotes islet innervation, but an absence of CST did not influence this.

We also studied the migration of bone marrow derived M1/M2 polarized macrophages towards different sympathetic nerves as well as different chemokine (LPS, MCP1 and CST) stimuli. Here we found that M1 macrophages migrated towards LPS and MCP1. Macrophages with the CKO genotype had a higher affinity towards MCP1 compared to wild type. M1 polarized macrophages seemed to have a higher affinity towards nerves that M2 polarized macrophages.

Finally, we looked at the potential difference in expression of macrophage markers using WT/WT, WT/CKO and CKO/CKO mice as well as the influence of duration of polarization. The different genotypes showed differences in gene expression. CKO/CKO lacked Adrb2 expression showing the importance of CX_3CR1 for nerve-macrophage interactions. It was found that pro-inflammatory and anti-inflammatory gene expression in macrophages changed over time.

This research enhances our understanding of the complex interactions between the immune system and nerves, which could be important for developing new treatments for T1D.

Acknowledgements

I am deeply grateful for all the opportunities and support provided by my thesis supervisor Gustaf Christoffersson, who not only afforded me the opportunity to conduct my thesis project within his esteemed group but also offered insightful feedback whenever it was needed.

My heartfelt appreciation extends to my co-supervisors:

- Elke M. Muntjewerff, whose extensive knowledge and readiness to answer my questions were crucial in shaping this work. Her continuous feedback and support during the writing process were immensely valuable.

- Vijay Sai Josyula, whose guidance and constant support in the lab were essential. I am grateful for his constant availability and willingness to assist whenever challenges arose.

I am also truly grateful to the entire Christoffersson lab team—Dali Epremidze, Myrthe Reiche, Hiromi Ikebuchi, and Robin Lindsay—for generously sharing their expertise and allowing me to observe and learn new techniques during experimental endeavors.

Furthermore, my sincere gratitude goes out to the members of the Mia Phillipson lab group, as well as my fellow student colleagues, support and the valuable experiences shared over the course of this past year.

Contents

1 Background

In this project, we focused on what influence macrophage-nerve interactions can have on the onset of type 1 diabetes (T1D) as well as the influence of nerves on islet macrophage behavior and migration.

T1D is an autoimmune disease which is characterized by an absence of insulin producing cells (beta-cells). It is thought that the development of T1D is caused by antigen presenting cells (APC) presenting peptides from β islets. These APCs get in contact with CD4+ T lymphocytes and these cells then activate autoreactive CD8+ T cells. The CD8+ T cells will lyse all beta cells in the islets that show this autoreactive peptide on their major histocompatibility complex (MHC) class I. Macrophages, natural killer cells (NK) and neutrophils will now release proinflammatory cytokines and reactive oxygen species to further destroy the β cells. It is thought that the CD4+ regulatory T cells (Treg) dysfunction in T1D causing the immune system to get out of control without any check (Hull, *et al*., 2017). Tregs are supposed to keep the immune system in check and prevent pathological self-reactivity. Activated T cells can subsequently stimulate B cells to respond to β cell proteins. The presence of circulating B cells that react to these proteins serves as a biomarker for Type 1 Diabetes (DiMeglio, *et al*., 2018).

Another potential cause for the autoreactivity resulting in T1D is thought to be a defect in the β-cells. The β-cells present an overexpression of HLA class I which could also be a cause of activation of the T cells. The cause of this upregulation is not known yet (Richardson, *et al*., 2016).

There is currently no cure for T1D, and treatment involves managing symptoms through insulin therapy and other medications. T1D is believed to result from a combination of genetic predisposition and environmental triggers. While certain genes can increase the risk of developing T1D, environmental factors, such as viral infections, may trigger the autoimmune response. T1D is not caused by diet or lifestyle, though these factors can influence disease management and overall health.

1.1 Macrophages

There are two types of macrophages, pro-inflammatory and anti-inflammatory. Tissue resident macrophages come from the yolk sac while Monocyte-derived macrophages differentiate from monocytes which come from the bone marrow. These monocytes circulate through the blood until they are needed somewhere after which they migrate into tissues. In the tissue they can differentiate into a macrophage or dendritic cell (McWhorter, *et al*., 2015).
Macrophages can be categorized into two main types (pro-inflammatory and anti-inflammatory) based on their receptor composition, secretion profile, and response to external stimuli.

Pro-inflammatory macrophages, also referred to as M1 or classically activated macrophages, are activated by interferon gamma (IFN-γ), tumor necrosis factor (TNF-α) or lipopolysaccharide (LPS). Macrophages produce pro-inflammatory cytokines (e.g., IL-1β, IL-6, IL-8, IL-12 and TNF-α) and chemokines (CCL2 and CCL5) which are involved in early-stage injuries, pro-inflammatory responses, and myoblast proliferation. Specifically, pro-inflammatory macrophages detect, engulf, and destroy bacteria through phagocytosis. Parts of the destroyed bacteria are presented on the outside of the macrophages by MHC allowing a T cell receptor to bind which in turn activates the adaptive immune response (Mills, *et al*., 2000).

Anti-inflammatory, referred to as M2 or alternatively activated macrophages, play an important role in tissue repair and anti-inflammation. They are activated by interleukin (IL)-4, IL-10, IL-13 or transforming growth factor-β (TGF-β), after which anti-inflammatory macrophages secrete anti-inflammatory cytokines (e.g., IL-10 and TGF-β), and other reparative factors needed for anti-inflammatory responses and repair and healing processes. To help with wound repair and vascular stability, the anti-inflammatory macrophages produce vascular endothelial growth factor (VEGF) and TGF-β1 (Mills, *et al*., 2000). M2 macrophages can be divided into four groups, M2a, M2b, M2c and

M2d of which each has a slightly different function. M2a macrophages are the main one mentioned in this report since they are found to be induced using IL4 and have an anti-inflammatory phenotype. Immunoregulation and tumor progression is mostly done by M2b macrophages and the M2c macrophages promote tissue repair/wound healing and phagocytose apoptotic cells. Lastly, M2d macrophages also have an anti-inflammatory function by producing IL10. These are activated by pro-inflammatory cytokine IL6 (Strizova, *et al*., 2023).

Depending on the location in the body, macrophages can have different functions. Macrophages in the pancreatic tissue are found to be notably different compared to the macrophages in the islets of Langerhans. Tissue macrophages are mostly anti-inflammatory macrophages while the macrophages found in islets are mostly pro-inflammatory macrophages (Calderon, *et al*., 2015). Islet macrophages are rarely produced by bone marrow/blood derived monocytes but come from definitive hematopoiesis. They express high levels of MHC class II, and cytokines like TNF-α and IL-1β. These islet macrophages are located next to blood vessels and in close contact with β-cells where they capture insulin containing granules and present these to autoreactive (diabetogenic) CD4 T cells. (Calderon, *et al*., 2015). Islets are not supposed to contain T cells, but research has shown that they will infiltrate the islets in the onset of T1D. Once in the islets, the T cells will attack and kill healthy insulin producing beta cells resulting in the dysfunction of islets. The reason for this infiltration varies between individuals and is a combination of environmental factors, genome, metabolism, and immune system (DiMeglio, *et al*., 2018).

Different studies suggest an increase of innate immune cells could have a causative and detrimental effect on the islet and β-cells in T1D (Böni-Schnetzler, *et al*., 2019). Diabetes mellitus (DM) is the result of immune mediated apoptosis of β-cells. High blood glucose levels can modify the monocyte/macrophage metabolism resulting in failures of the innate immune system and inflammatory mechanisms. Different research suggests that DM promotes the inflammatory monocyte/macrophage phenotype causing pancreatic islet inflammation and β-cell dysfunction (Ying, *et al*., 2019).

Research shows pathological changes in the pancreas, like an increase of MHC class I expression in β-cells before a patient shows the clinical signs of T1D (Coppieters, *et al*., 2012). It is not yet known why this elevation of MHC class I expression happens, but it seems to go with an elevation of CD8+ T cells in the islets (Rodriguez-Calvo, *et al*., 2015).

Autoreactive CD8 T cells are even found in peripheral blood of healthy individuals. However, the frequency of autoreactive beta-cell specific CD8 T cells in T1D patients is a lot higher compared to healthy individuals (Velthuis, *et al*., 2010).

1.2 Nerve-associated macrophages

A specific kind of tissue macrophages are associated with the peripheral nervous system (PNS). Tissue-resident macrophages are found in different tissues throughout the body and play a role in immune surveillance and tissue homeostasis (Davies, *et al*., 2013) while nerve-associated macrophages (NAMs) specifically reside near nerves and are involved in maintaining nerve health and function (Kolter, *et al*., 2020). Both types of macrophages are involved in immune responses, nerve-associated macrophages have specialized functions related to supporting nerve tissue.

The prevalence of these NAMs is very low compared to other tissue macrophages. While NAMs are adapted to the specific tissue they occur in, they all are morphologically similar and highly express CX_3CR1 also known as the fractalkine receptor. The fractalkine receptor can be used to identify NAMs in different tissues. However, there are other macrophages which also produce fractalkine receptor, like interstitial macrophages (IMs). Interestingly, IMs are not derived from original nerve-resident

macrophages or from circulating macrophages but seem to be capable of upregulating CX_3CR1 when in close contact with unoccupied nerve axons. This would suggest NAMs differentiate on cues they get from the PNS (Kolter, *et al*., 2020). The signal cascade of CX_3CR1 stimulates cells in a higher active state and recruits immune cells via chemotaxis and diapedesis. This cascade is also associated with different disease pathophysiology.

1.3 Innervation of the pancreas

An important job of the pancreas is to regulate the glucose homeostasis. This is done by a complex interaction between different organs. The production of glucose is triggered in the liver by hormones coming from the pancreas. The liver produces glucagon when glucose levels are too low, helping to stabilize glucose fluctuations in the body. In response to high glucose levels the gastrointestinal tract will release hormones (e.g. adrenaline) to trigger the pancreas to release insulin. The brain also plays an important role in glucose homeostasis by releasing signals through the sympathetic and parasympathetic nervous system in case of food intake or stress (Rodriguez-Diaz, *et al*., 2014).

The pancreas houses a lot of nerves which are important for the homeostasis of the pancreas including secretion of pancreatic enzymes. Acetylcholine, released by the intrinsic nerve fibers, triggers the release of insulin from the β-cells. Secretion of insulin triggered by parasympathetic neurotransmitters can be inhibited by sympathetic neurotransmitters (Ahren, 2000), (Bockman, 2007). Rodriguez-Diaz, *et al*., found that human islets were mostly innervated by sympathetic nerves targeting endocrine cells. These tyrosine hydroxylase (TH)+ nerves were mainly located along the blood vessels innervating smooth muscle cells. (Rodriguez-Diaz, *et al*., 2011).

Mundinger *et al*. found that T1D patients have a selective loss of sympathetic nerves in the pancreatic islets during the early onset of the disease as well as with long-term durations. This loss in nerves was found to be specific to T1D and not present in T2D, suggesting that this loss of nerves is triggered by the autoimmune attack (Mundinger, *et al*., 2016). It is also found that denervation halts the onset of T1D in mice specifically bred to develop T1D (Christoffersson, *et al*., 2020). Glucagon secretion plays an important role in managing hypo- and hyperglycemia in diabetes patients. The loss of nerves may account for the impaired glucagon secretion in T1D in response to hypoglycemia (Campbell-Thompson, *et al*., 2021).

1.4 CX_3CR1

CX_3CL1 (fractalkine in humans and neurotactin in mice) is a pro-inflammatory chemokine from the CX_3C family that binds to CX_3C motif chemokine receptor, fractalkine receptor or G protein-coupled receptor 13 (GPR13). CX_3CL1-CX_3CR1 binding helps in cell recruitment, cell survival and cellular adhesion (Aoyama, *et al*., 2010). Neurons in the central nervous system (CSN) express CX_3CL1 as a membrane-bound protein. Through proteolysis by enzymes like ADAM10 and ADAM17, CX_3CL1 is cleaved, leading to the formation of a soluble form known as fractalkine (FKN) (Gregg, *et al*., 2014). FKN is expressed on endothelial cells and lymphocytes as well as on the spinal neurons and sensory afferents while CX_3CR1 is expressed on a wide area of cell types which include natural killer (NK) cells, cytotoxic T cells, monocytes/macrophages, B cells, smooth muscle cells, tumor cells and microglia (Sindhu, *et al*., 2017). The soluble form of FKN attracts T cells and monocytes while the cell surface bound protein promotes a strong adhesion for leukocytes (Tsubota, *et al*., 2009).

The interaction between CX_3CR1 and FKN play a crucial role in mediating communication between neurons and macrophages. CX_3CR1 helps to maintain the balance between neuronal activity and immune responses by regulating the recruitment and activation of macrophages in the nervous system. This interaction is essential for neuronal maintenance, synaptic plasticity, and immune surveillance in the central nervous system (Cardona, *et al*., 2006). Dysregulation of CX_3CR1-mediated

nerve-macrophage interactions can lead to neuroinflammation and neuronal damage (Imaj, *et al*., 1997).

1.5 Catestatin

Chromogranin A (CgA) is a secretory protein found in neuroendocrine cells throughout the body, especially in the adrenal glands, pancreas, and gastrointestinal tract (Mahapatra, *et al*., 2005). It is produced, stored, and released in the adrenal glands along with catecholamines like norepinephrine (Shah, *et al*., 2012). CgA is often used as a biomarker in the diagnosis and monitoring of neuroendocrine tumors (NETs) and other tumors originating from neuroendocrine cells (Mahapatra, *et al*., 2005). Mahpatra, *et al*., also found, using CgA knock out mice, that CgA could have a regulatory effect on blood pressure. CgA has been found to inhibit glucose-induced insulin release and to contribute to the pathogenesis of T1D (Tatemoto, *et al*., 1986). Baker *et al*. suggest the presence of CgA and the hereby activated CgA reactive T cells to be essential for the initiation and development of T1D in non-obese diabetic (NOD) CgA knock out (KO) mice (Baker, *et al*., 2016). The neuropeptide catestatin (CST), a cleavage product from CgA, possibly has a role in the development of T1D since CgA and thus CST are produced in the beta cells of pancreatic islets (Bartolomucci, *et al*., 2011). CST not only inhibits the release of catecholamine (CA) by binding to the nicotine acetylcholine receptor on adrenal medullary chromaffin cells or adrenergic neurons (Mahapatra, 2008) but also suppresses the secretion of neuropeptide Y, adenosine triphosphate (ATP), and CgA. The action of CST is proposed to be associated with blockage of calcium ion (Ca^{2+}) influx suppressing CA (adrenaline, noradrenaline, and dopamine) release and the CgA gene (CHGA) transcription (Bralewska, *et al*., 2024). CST has also been found to have an anti-inflammatory function by reducing pro-inflammatory macrophage markers IL-6, IL-1β and TNF-α levels and expression with CST treatment (Ying, *et al*., 2018).

CST is proposed to be produced by macrophages and play an important role in an anti-inflammatory feedback loop to suppress macrophage-driven inflammation (Muntjewerff, *et al*., 2021).

1.6 Neuro-immune interactions in kidneys, lungs and heart

In 2000 Borovikova *et al*., found that the main nerves of the parasympathetic nervous system also known as the vagus nerve plays an important role in the immune system. The vegus nerve has innervated different organs and can regulate the function of them. By using LPS, they made an inflammation model resulting in the release of TNF-α by the vegus nerve (Borovikova, *et al*., 2000), suggesting that this nerve directly regulates the activity of the immune system (Hasegawa, *et al*., 2019).

The lungs are a vital part of the first line of defense against pulmonary infections. They have a big epithelial surface connected to the external environment causing them to be a target for airborne pathogens. T cells residing in the lungs play an important role to protect the body, however there are other resident innate immune cells working hard to protect.

There are two types of macrophages in the lungs, interstitial macrophages (IMs) and alveolar macrophages (AMs). IMs present only 4% of all macrophages present in mouse lungs and commonly reside in the interstitium together with dendritic cells (DC) and lymphocytes. Of these two types of macrophages, only IMs (CD169+ and CD169-) are found to express CX_3CR1 (Sabatel, *et al*., 2017, Ural, *et al*., 2020). These IMs were found to be embryonically derived through the yolk sac and in close interaction with tyrosine hydroxylase (TH) expressing nerves and beta-tubulin, supporting the conclusion that these cells can be called NAMs. Ural *et al*., also found that lung nerve- and airway associated macrophages have a high expression of C1qa, C1qb, C1qc (classical triggered complement cascade genes), MHC class II, Mgl2, CD83, Apoe, Pf4 and Tmem176a as well as a dependency of CSF1-CSF1R for their development and/or survival. NAMs in the lungs were found to be the main producer

of anti-inflammatory cytokine IL10, while AMs were found to be of importance in clearing infections and thus stimulating inflammation. This suggests the importance of NAMs in regulating the inflammation response and prevent tissue damage (Ural, *et al*., 2020).

Kidneys are highly innervated organs receiving signals from the sympathetic nervous system. The sympathetic nerves are mainly found around the arteries in the kidneys. Excitation from the sympathetic nerves result in an increase of norepinephrine (NE) release. NE can bind to α1B and α1 adrenic receptors. Activation of the α1B receptor promotes the activity of NA^+, K^+, and 2 Cl^- cotransporters, while activation of the α1 receptor increases the activity of NA^+ and H^+ protein pumps. Which in turn causes an increase of sodium and water reabsorption of the kidneys leading to acidification of the urine as well as a decrease in the blood flow (Zhu, *et al*., 2023) (Hasegawa, *et al*., 2019). When the kidneys were denervated, there was a significant reduction in kidney inflammation and macrophage infiltration (Banek, *et al*., 2019). However, inflammatory levels went back up when norepinephrine (NE) was reintroduced to the denervated kidneys. NE reintroduction led to an increase in macrophage and neutrophil infiltration in the kidneys (Gauthier, *et al*., 2023).

A group of bone marrow independent macrophages originating from the embryo have been found in the kidneys. These self-maintaining (SM) macrophages have been found to highly express nerve associated genes (Maoa, Npy1r and Slc6a2) and suppress genes associated with metabolism and molecule transport (Zhu, *et al*., 2023). In cases of acute kidney injury, it has been found that macrophages play a role in repair by secreting IL-22 (pro-regenerator) and colony-stimulating factor 1 (CSF-1). CSF-1 is important to polarize macrophages into their M2, anti-inflammatory phenotype. The specific interactions of macrophages with other cell types in case of kidney damage repair is still unclear (Chen, *et al*., 2022). CX_3CR1 can serve as a marker for kidney macrophages. Within the kidney, CX_3CR1+ macrophages are crucial for immune surveillance and tissue homeostasis. Fractalkine was found to significantly increase after depletion of kidney macrophages, suggesting that fractalkine is released in the kidneys to attract new monocytes after it loses its macrophages (Liu, *et al*., 2020).

When the heart is healthy, the cardiac macrophages are similar to anti-inflammatory macrophages which are important to maintain homeostasis. Mice have 4 different cardiac macrophages which are based on MHCII and CX_3CR1 expression. Two of which are either positive for MHCII or CX_3CR1, one that is negative for both and one that is positive for both. The number of macrophages per population is age dependent. At birth almost all macrophages are $CX_3CR1^+MHCII^-$ and with age the CX_3CR1^+ macrophages disappear and the $MHCII^+$ macrophage population increases (Ma, *et al*., 2018). Macrophages may potentially contribute to cardiac aging, suggesting that as mice age, there could be an increased presence of macrophages in the heart (Chiao, *et al*., 2011).

2 Methods

2.1 Mice

For the following experiments female C57BL/6 GFP wildtype (WT) CX_3CR1 +/- and CX_3CR1 KO GFP (CKO) CX_3CR1 -/- mice were used. The mice were anesthetized using isoflurane which was checked by pinching the toes after which they were sacrificed by dislocating the neck. All animal experiments were approved by the regional animal ethics committee of the Uppsala region, Sweden.

2.2 Tissue harvesting and sectioning

Various organs (heart, lungs, kidneys and pancreas) were harvested from 3 female GFP wildtype (WT), CX_3CR1 +/- and CX_3CR1 KO GFP (CKO) CX_3CR1 -/- mice. After harvesting, the organs were fixated in a 4% paraformaldehyde solution for 24 hours (h). After fixation, the paraformaldehyde solution was drained, and the organs washed with PBS (DPBS from Gibco, Ref: 14190-094) after which the organs were saturated in a 15% sucrose solution for 24 h. Next the organs were saturated in a 30% sucrose solution for 48 h. Finally, the prepared organs were embedded in Neg-50 compound (Ref: 6502, epredia) and sliced in 30 µm thick sections with a cryostat, put on microscope slides (Ref: J1800AMNZ, epredia). Slides were stored at -20 ^{o}C until staining.

2.3 Slide staining

Before staining the heart, heat induced antigen retrieval (AR) using a pressure cooker was performed. This method is used to break the bonds between formalin and proteins. Breaking this bond allows antibodies to reach the target protein in the tissue. First, the slides were thawed at rt for 15 minutes (min) after which they were put in a citrate buffer in a pressure cooker for about 20 min. After this, the slide staining protocol was followed for all tissues.

First tissue slides were thawed for 15 min at room temperature (rt). While thawing, the tissues were surrounded by a hydrophobic barrier with a Vectra PAP ImmEdge pen (Cat# H-4000, Lot: ZJ1031 from Vector Laboratories). Next, the slides were washed in PBS two times for five min each. Afterwards, they were rehydrated for 10 min in 1xPBS+0.2% Tween (PBST). After rehydrating, the slides were dried and 200 µL of 0.2% triton-x100 was added per slide and incubated for 10 min at rt. The slides were washed again in PBST for five min after which 200 µL MAGIC buffer protein blocker (dPBS+0.2%Saponin+0.1%NA Azide+2%FBS) was added to each slide and incubated for 30 min. The primary antibody solutions were prepared in MAGIC buffer and 200 µL of this mixture was added per slide and left to incubate overnight at 4 ^{o}C. The pancreas was first completely stained with insulin (primary and secondary antibody) before staining for nerves and macrophages. This was done with guinea pig insulin antibody 1:1000 (GeneTex, Lot: 822101934) incubated overnight as written above and anti-GP AF 488 (Invitrogen, Ref: A11073) was used as a secondary antibody 1:1000. For sympathetic nerves tyrosine hydroxylase (TH, Abcam rabbit anti mouse, AB 112) 1:100 was used and as macrophage marker, F4/80 (rat anti mouse, Invitrogen Ref: 14-4801-85) 1:200 was used for kidney tissue and ionized calcium binding adaptor molecule 1 (IBA1, SYSY, rat anti mouse, Ref: 234017) 1:500 was used for lung, heart and pancreatic tissue. Rabbit norepinephrine transporter (NET) (Abcam, Ref: 254361) was used 1:200 on pancreatic tissue as a nerve marker. To prevent the tissues from drying during incubation, water was added to the staining box. After incubation, the slides were washed three times with PBST for five min each. While washing, the secondary antibody solution was prepared in MAGIC buffer. For the nerve staining Alexafluor 555 donkey anti rabbit (Invitrogen, Ref: A31572) 1:100 for kidneys, lungs and heart and 1:1000 for pancreatic tissue was used and for the macrophage staining Alexafluor 647 donkey anti rat (Invitrogen, Ref: A48272) 1:200 for F4/80 and 1:1000 for IBA1 were used. 200 µL of this mixture was added to each slide for 60 min for kidneys and 120 min for lungs and heart at rt. The slides were washed three times for five min with PBST after which they were dried.

Next 200 µL per slide of Hoechst 33342 (1:10.000) was used to stain the cell nuclei. After 10 min incubation at rt, the slides were washed two times in PBST and once in PBS for five min each. The slides were properly dried, and two drops of Prolong Gold antifade reagent from Invitrogen Thermo fisher scientific (Ref: P36934) were applied to each slide. The coverslip was gently placed with an angle and air bubbles were removes by using tweezers. The slides were left to dry for at least 60 min at rt in a staining box with some dry paper tissues after which they were stored at 4 °C until imaging.

2.4 Confocal imaging

Pictures of the fixed tissue slides were made with a TCS SP8 Leica confocal microscope using objective L 25x/0.95 W visar (Lot: 506374) and were analyzed afterwards using Imaris. In Imaris, the nerve-macrophage network was analyzed by looking at the macrophage and nerve areas and the overlay of these signals. The following settings were used for the nerve and macrophage analyses: background subtraction of 2.00, service details: 0.670 and the filter type was volume. For the tissue surface analyses, the standard settings were used. The threshold was changed to only cover nerves/macrophages when needed and the results were obtained via the statistics in Imaris. All data obtained with Imaris was normalized in Excel by dividing the nerve/macrophage volume by the volume of the nucleus staining.

2.5 ImageJ image analyses

Slide scans of the pancreas were analysed using ImageJ to obtain the staining intensity. The islets were identified with QuPath after which they were exported to ImageJ using the in-app options. In ImageJ, the different channels were split from each other after which the Hoechst staining got the IsoData, insulin staining the Shanbhag, nerves (NET) Minimum dark and macrophages (IBA1) MaxEntropy. The measurements of the staining intensity from the macrophage and nerve staining were compared to each other in WT, CST-KO and CgA-KO mice.

2.6 Macrophage isolation and culture

Macrophage specific gene expression was observed by isolating macrophages and exposing them to various stimulants.

Macrophages were obtained from the bone marrow of the hindlegs of mice. Four bones per mouse were collected, two hind legs with each an upper and lower leg bone. This was done by sacrificing the mouse via cervical dislocation after anesthetizing the mouse and isolating the bones of the hindlegs. All bone marrow of one mouse can be collected in one tube. Both ends of a bone were cut off to be able to flush the marrow out above a 50 mL falcon tube containing a 40µm nylon filter with PBS using a 27Gx¾"(0.4x10 mm) needle and 1 mL syringe. Bone marrow staying on the filter was grinded through with the end of a clean syringe and flushed with PBS (about 5 mL end volume). Next, the cells were centrifuged at 1500 rpm at 4 °C for 5 min and kept on ice. The supernatant was discarded, and 3 mL lysis Ack buffer (Ref: A10492-01 from Gibco) was added to the pallet to lyse the red blood cells. This mixture was incubated for 2 min on ice after which 7 mL cell culture media (RPMI) was added. The tubes were then centrifuged again at 1400 rpm at 4 °C for 5 min after which the supernatant was discarded. 50 mL of media and 12.5 µL MCSF (Lot# 0122245 K3022) was added per tube. After proper mixing, 25 mL media was added per plate. The media was spread over the plate by moving it left to right and up and down (NO swirling, this collects all cells in the centre of the plate). The plates were incubated at 37 °C for 48 h with 5% CO_2.

After 48 h the growth of the macrophages was checked and if the bottom of the plate was covered for 60-80%, they were split into new plates to prevent cell death by overgrowth. If this was not the case, the media was changed to prevent the cells from starving.

2.7 Macrophage polarization

As many macrophages as possible were gently scraped off the bottom of the plate. After pipetting the media around over the plate, all media was collected into a 50 mL falcon tube. Plates containing macrophages from the same condition (WT or KO) were combined into one tube. All tubes were centrifuged at 1400 rpm at 4 °C for 5 min, after which the supernatant was discarded. After loosening the pallet, 10 mL media was added per tube. Now the cells were counted to be able to approximately add the same number of cells per well in a 6 wells plate. The aim was to get $0.6x10^6$ cells per well (3 mL media). 0.25 µL MCSF/mL was added to the media and the cells were incubated for 48 h at 37 °C with 5% CO_2.

M0 macrophages were polarized into inflammatory and anti-inflammatory macrophages (M1 and M2). IFN-gamma Lot# 061798 L2117 from PeproTech (0.2 µg/mL) and LPS (100 µg/mL) was used to stimulate M0 macrophages to polarize into M1 macrophages and IL4 Lot# 021749 C1218 (0.2 µg/mL) was used to polarize M0 into M2 macrophages.

First, media per well was prepared to prevent the cells from staying dry for too long. The following was added per well (3 mL media). For M1, 0.6 µL IFN-gamma (stock 20 µg/mL) and 3 µL LPS (stock: 100 µg/mL) was added and for M2, 0.6 µL IL4 (stock 20 µg/mL) was added. 2.5 µL MCSF (stock: 100 µg/mL) was added per 3 mL media per condition. The old media was aspirated from the cells and 3 mL per well of the newly prepared media was added. After 24 h at 37 °C with 5% CO_2, the M1 macrophages were round and small and the M2 macrophages stretched out.

2.8 Migration assay

A migration assay was used to study the migratory capacity of bone marrow derived macrophages isolated from WT and CKO mice using transwell plates.

First, the macrophages were scraped off the plates, on which they were polarized. The cells were pooled together according to their cell type resulting in M0, M1 and M2 of both WT and CKO. Next, the cells were washed once in PBS at 300 G for 5 min at 4 °C after which they were resuspended in 1 mL cell culture media. The cells were counted here and spun again to then resuspend the cells such that there were $2.5x10^5$ cells for the chemokine experiment and $3x10^5$ per 100 µL media. Cell growth media containing different chemokines per condition was prepared. One with LPS, one with 10 ng/mL MCP1 (stock 100ng/mL, PeproTech Lot# 0510126), one with CST (1:500) and a blanc. 250 µL of this media was added per well following the schematics shown in figure 1.

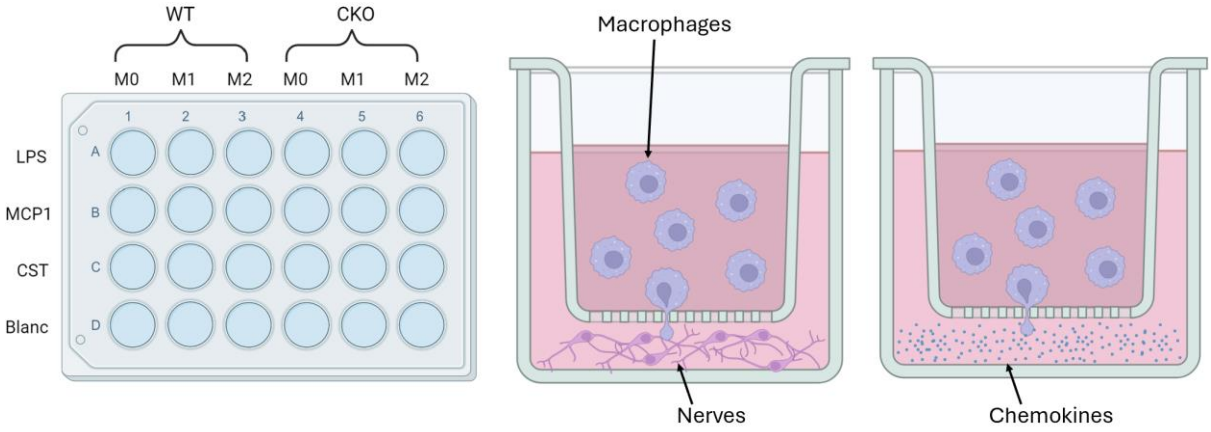

Figure 1: Transwell migration plate layout to the left and to the right a schematic overview of the assay with macrophages in the filter on top and either nerves or chemokines as attractants on the bottom, Biorender.

100 µL of the cell suspension was pipetted onto the filter and the filter was placed on top of the chemokine media following figure 1. After 24 h incubation the cells were collected from each well and transferred to a 96 well plate. The plate was centrifuged at 300 G for 3 min and the supernatant was discarded. Next the cells were washed with PBS and centrifuged again at the same settings. After this, the cells could be prepared for flow to count the number of migrated macrophages.

To prepare for flow, the cells were stained with 1:1000 live dead aqua (Invitrogen Lot# 1802492) and incubated for 20 min at 4 °C after which they were centrifuged at 300 G for 3 min discarding the supernatant. The cells were washed with 100 µL FACS buffer per well, centrifuged again, and suspended in 120 µL FACS buffer before running flow.

2.9 Fractalkine stimulation and RNA isolation

Macrophages were stimulated with different concentrations of fractalkine Lot# 1105106 E1822 from PeproTech with a stock of 100 µg/mL (FKN). Before use, the media was heated up to 37 °C. Next, media solutions with different concentrations FKN were prepared. The media of the cells was aspirated, and the cells were washed with PBS for about 5 min with periodically mixing. After aspirating the PBS, 2 mL prepared media with FKN and M-CSF was added per well. After 24 h of incubation at 37 °C with 5% CO_2, the mRNA was isolated using a Norgen Biotek corp Single cell RNA purification kit (product # 51800) following the hereby provided protocol from the manufacturer. For the final step, 18 µL elution solution A was used resulting in 18 µL RNA.

2.10 Reverse transcription

The RNA concentration was measured using a nanodrop 2000 from Thermo scientific. For the reverse transcription, 0.05 µg RNA/sample was used in 13.2 µL H_2O. This was done to ensure all samples had a comparable RNA starting concentration. Next, a cDNA master mix (MM) was prepared using the High-Capacity cDNA Reverse Transcription Kit (Ref: 4368814) from applied biosystems by Thermo Fisher Scientific and the protocol provided by the manufacturer. According to the protocol, 6.8 µL MM was added to the diluted RNA resulting in a reaction volume of 20 µL per sample. The kit was used in combination of RNase Inhibitor, Ref: N8080119. The kit also comes with a protocol for the thermal cycler, which was used for the reverse transcription.

All obtained cDNA was diluted 1:5, cDNA:H_2O. For this qPCR, 5 µL/sample Fast SYBR Green Master Mix from applied biosystems by Thermo Fisher Scientific (Ref: 4385612) was used combined with 2.8 µl/sample H_2O and 0.1 µL/sample for each the forward and reverse primer (Table 1). The qPCR was performed using a 384 wells plate and in each well, 8 µL of the prepared MM and 2 µL of the diluted cDNA was added.

Tabel 1: PCR primers

GAPDH	Fw: TGTGTCCGTCGTGGATCTGA	Actb	Fw: CTCTGGCTCCTAGCACCATGAAGA
	Rev: CCTGCTTCACCACCTTCTTGAT		Rev: GTAAAACGCAGCTCAGTAACAGTCCG
IL6	Fw: TAGTCCTTCCTACCCCAATTTCC	IFNg	Fw: TCAAGTGGCATAGATGTGGAAGAA
	Rev: TTGGTCCTTAGCCACTCCTTC		Rev: TGGCTCTGCAGGATTTTCATG
Nos2/iNOS	Fw: CCCTTCAATGGTTGGTACATGG	IL4	Fw: GGTCTCAACCCCCAGCTAGT
	Rev: ACATTGATCTCCGTGACAGCC		Rev: GCCCATGATCTCTCTCAAGTGAT
IL10	Fw: TGGCCCAGAAATCAAGGAGC	Mgl1	Fw: AACCTCCAGAACTCAAGGATCG
	Rev: CAGCAGACTCAATACACACT		Rev: AGCTTTACCAGGCTCTTGGGT
Arg1	Fw: GAATCTGCATGGGCAACC	Mgl2	Fw: CAGAACTTGGAGCGGGAAGAG
	Rev: GAATCCTGGTACATCTGGGAAC		Rev: TTCTTGTCACCATTTCTCATCTCCT
TNFa	Fw: GAGAAAGTCAACCTCCTCTCTG	F4/80	Fw: CCCCAGTGTCCTTACAGAGTG
	Rev: GAAGACTCCTCCCAGGTATATG		Rev: GTGCCCAGAGTGGATGTCT
Adra1a	Fw: GGCTCAGGAGAGACTTTCTA		
	Rev: TTGGTCCTTCGGCATGGTAA		
Adrb2	Fw: TGGTGGTGATGGTCTTTGTC		
	Rev: GTCTTGAGGGCTTTGTGCTC		
MMR/Mrc1	Fw: CCACAGCATTGAGGAGTTTG		
	Rev: ACAGCTCATCATTTGGCTCA		

2.11 Statistics

A significant difference was considered for anything with a p value below 0.05. GraphPad Prism 10 was used for the statistics. Here the outliers of the data set were identified with an outlier test and excluded first and, after ensuring the data was not normally distributed, a Mann-Whitney test was performed for the colocalization experiment.

To normalize the data after the qPCR, the Ct of the housekeeping gene, GAPDH, was subtracted from the Ct of the other genes. The data was statistically analysed using an ANOVA test.

3 Results

3.1 CX_3CR1 absence results in less nerve-macrophage interactions in lungs and kidneys

To measure nerve and macrophage colocalization in the kidney, lungs and heart, tissues were stained for F4/80 to identify the macrophages and tyrosine hydroxylase (TH) to visualize the sympathetic nerves.

Four controls were used with each staining. One WT pancreas with the same staining as the experiment slides since this experiment is already done in this lab on pancreas and known to work. Two WT control samples were included in the staining protocol. One control was treated with only secondary antibodies to confirm that there was no staining in the absence of a primary antibody. The other WT control was stained specifically for either nerves or macrophages to assess for any cross-staining. Both controls were not treated with Hoechst dye. Lastly, one CKO tissue was stained only for Hoechst, and one was not stained at all but would be expected to have a GFP signal since GFP+ mice were used.

However, no F4/80 signal was not found in the lungs (figure 2A). To still be able to stain the macrophages in the lungs, IBA1 was instead used as a marker for macrophages in the following experiments for the lungs and the heart (figure 2B). GFP mice were used making it possible to observe GFP expressing macrophages in the tissue. These GFP expressing macrophages served as a control and were present in the tissue were no F4/80 macrophages were observed.

According to Zaynagetdinov *et al.,* 2012, macrophages in the lungs have a weak F4/80 expression. Following this finding, the antibody was changed and IBA1 macrophage marker was used for the lung sections as well as the heart.

It proved to be difficult to stain for either the macrophages or nerves in the heart as shown in figure 2b. A way to overcome this is to perform antigen retrieval. This resulted in a better nerve and macrophage staining compared to the staining done without antigen retrieval. Since this method proved to work, no other methods were tried. The antigen retrieval was not performed with the other tissues since there was no problem with staining.

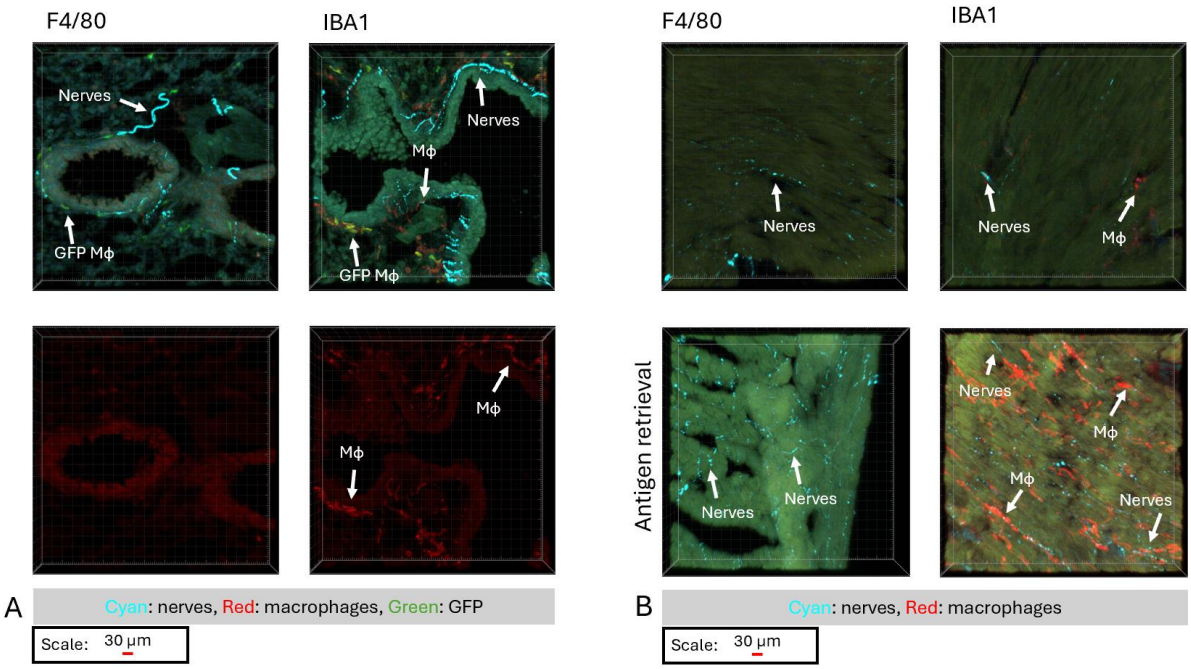

Figure 2: Optimalization of staining protocol, A: WT lung tissue showing F4/80 (left) and IBA1 (right) macrophages (red) with GFP macrophages (green) as control. White arrows indicate nerves and macrophages. B: WT heart tissue comparing with (top) and without (bottom) antigen retrieval and F4/80 (left) and IBA1 (right) macrophages. All sections were 30 µm thick.

After optimizing the macrophage staining for each organ, we continued with staining of the lungs and heart (figure 3 A-F). Here the nerves were represented by the cyan colour and the macrophages are shown in red. WT kidneys and lungs showed a greater macrophage volume (figure 3 G2 and H2) and more colocalized volume per tissue volume (figure 3 G1 and H1) as well as a greater colocalized volume per nerve volume (figure 3 G3 and H3) compared to CKO. For heart tissue we found a greater macrophage volume in CKO mice compared to WT mice (figure 3 I2). There was however no difference in colocalized volume per tissue volume observed (figure 2 I1). The colocalized volume per nerve volume was greater in CKO mice compared to WT mice in the heart (figure 3 I3).

In the kidneys and lungs, WT mice had a significantly higher colocalization of nerves and macrophages compared to the CKO mice (figure 3G, 3H). This suggests that an absence of CX_3CR1 results possibly in less nerve-macrophage association in these organs. In the heart, the opposite results were found: a higher colocalization in CKO mice compared to WT mice. There was no difference in the innervation (supplement IA) between WT and CKO mice but an increase of IBA1 macrophages was observed in the CKO mice compared to WT. This could be the reason for a higher colocalization per nerve volume (supplement I B) in the CKO. The macrophage increase would suggest an inflammation reaction possibly caused by the CX_3CR1 KO. However, since there is no previous data available about IBA1 expression in CX_3CR1 macrophages more research is needed.

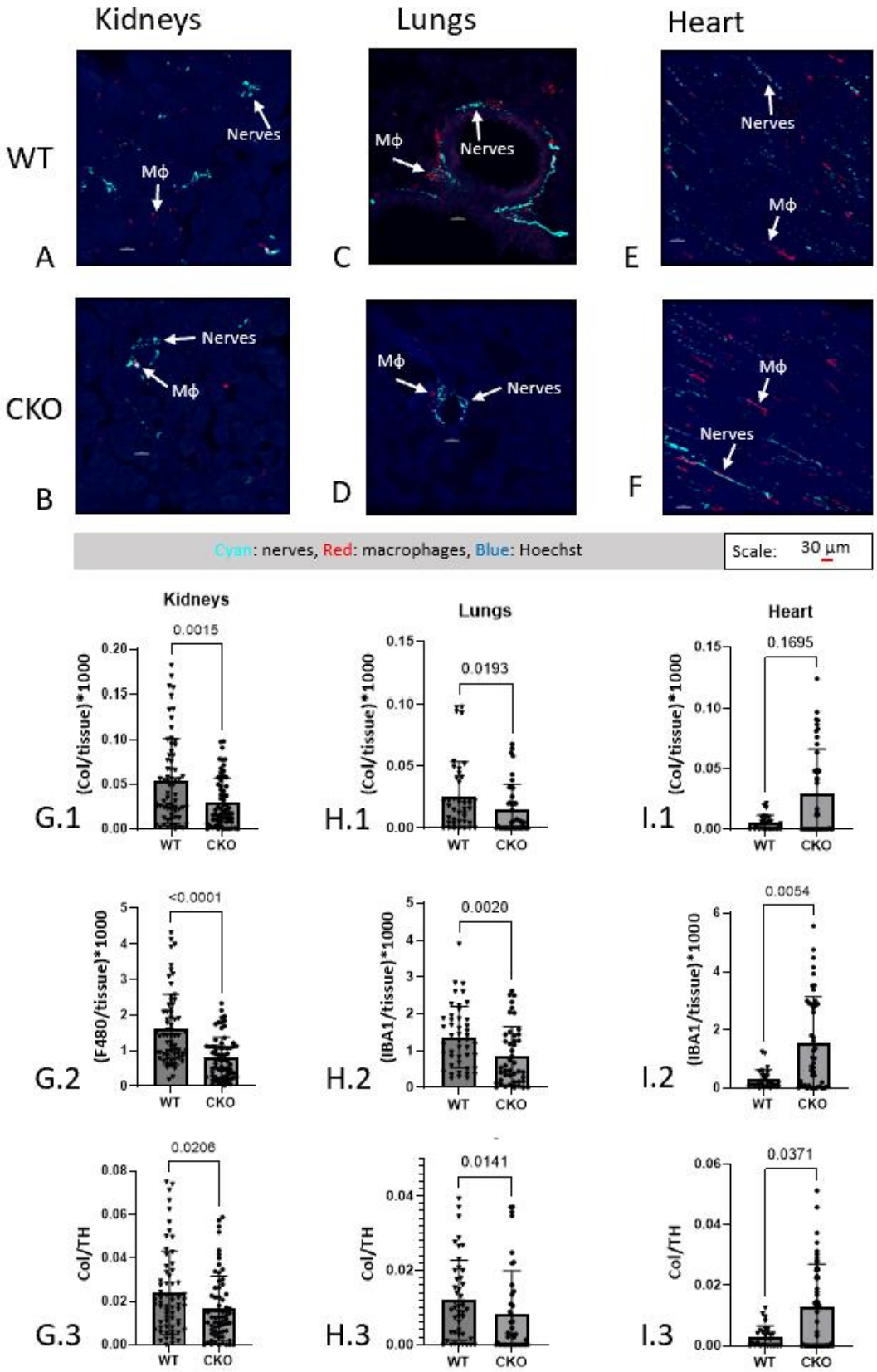

Figure 3: Nerve-macrophage staining. A and B: F4/80 macrophages in red and sympathetic nerves (TH) in cyan for WT (CX_3CR1 +/-) and CKO (CX_3CR1 -/-) in kidney, C-D lungs and E-F heart with IBA1 macrophages in red. G1-I3: WT and CKO on the x-axis. G1: Colocalization of nerves and macrophages on the y-axis divided by the total tissue volume in kidney, H1 lungs and I1 heart. G2: Amount of macrophage volume/tissue on the y-axis divided by the total tissue volume in kidney, H2 lungs and I2 heart. G3: Colocalized volume/nerve volume on y-axis, H3 lungs and I3 heart. All sections were 30 µm thick. Statistics: N=3, analyzed with ANOVA, significant difference: $p < 0.05$.

3.2 CgA-KO mice have a higher nerve ratio per islet compared to WT and CST-KO

Another staining experiment was performed on CgA-KO and CST-KO mice to measure the macrophages and nerves per islet. The macrophages were stained for IBA1 and the nerves for NET. Islets were identified with an insulin and Hoechst staining (Figure 4).

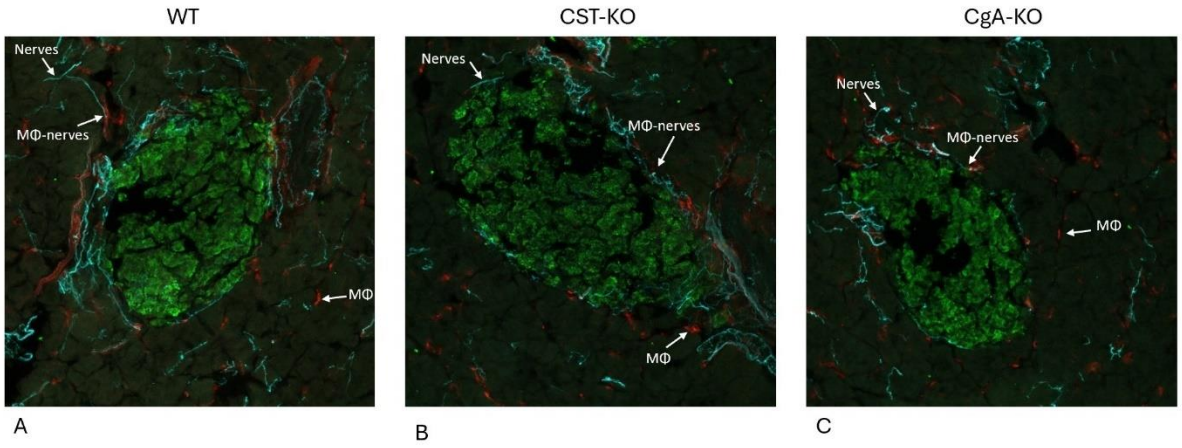

Figure 4: Nerve-macrophage staining of the pancreas. IBA1 macrophages in red, NET nerves in cyan and green shows insulin producing cells. The figure shows the insulin producing islets in A: WT mice, B: CST-KO mice and C: CgA-KO mice. All sections were 30 µm thick.

Figure 5C shows that CgA-KO had a higher nerve ratio per islet area compared to the WT and CST-KO samples. CST is a neuropeptide and a cleavage product from CgA. The results show no difference between WT and CST-KO, suggesting that an absence of CgA promotes innervation of the islets but an absence of CST has no influence on the islet innervation according to this experiment. The other graphs show no significant difference, however figure 5A and 5B show a trend in reduction of macrophages per islet and macrophage colocalization with nerves per islet. when comparing WT with CgA-KO and CST-KO.

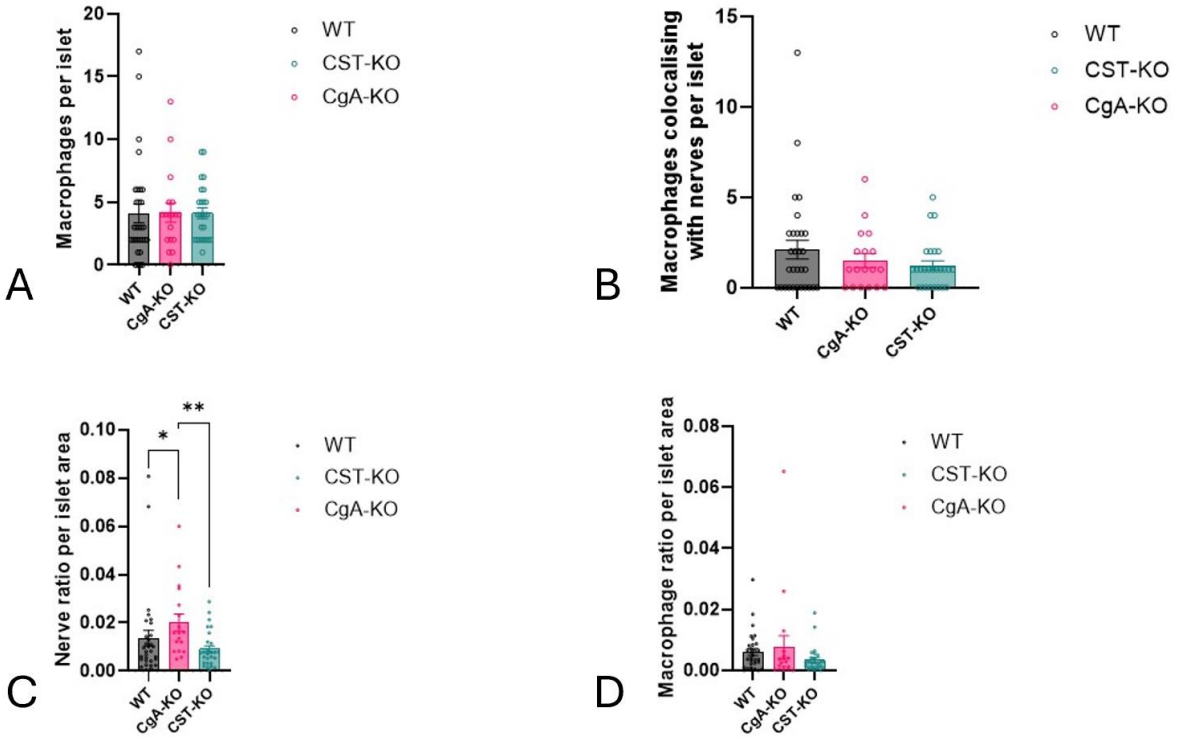

Figure 5: Macrophages were stained with IBA1 and the nerves were stained with NET. WT, CgA-KO and CST-KO on the X-axis. A: Counted macrophages per islet on the Y-axis, B: Macrophage colocalization with nerves per islet on the Y-axis. C: Nerve ratio per islet area measured with staining intensity. D: Macrophage ratio per islet area measured with staining intensity. All sections were 30 µm thick. Statistics: N= 31 for WT, N= 27 for CgA-KO and N= 18 CST-KO, significant difference: $p < 0.05$.

3.3 Migration assay

The migration of bone marrow derived macrophages towards different chemokines (LPS, MCP1 and CST) and nerves was measured using flow cytometry. These are preliminary data; the results represent one experiment with N=1. In this experiment, the data was gated for total cells → single cells → live cells (figure 6A). A single cell gate was needed to separate out all the cells that stick together. Since this little clump consists of two cells, it will also give a signal twice as high.

When looking at the total of migrated single cells, not the live cells, figure 6B shows a high number of M1 macrophages migrating towards LPS both for WT and CKO phenotypes. A lower migration rate towards LPS in M2 macrophages was expected since LPS activates M1 polarization. However, Zheng, *et al*., found that LPS can transform M2 macrophages towards a M1 phenotype, giving a possible explanation for the towards LPS migrated M2 macrophages (Zheng, *et al*., 2013). It would be interesting to perform a qPCR on these samples to check which genes are expressed.

The live/dead gating showed a lot of cell death among the total of migrated macrophages (figure 6B, orange dots). This experiment was performed over a 24h timeframe which is in comparison to migration assays of other groups which varied between 2 – 5h (Justus, *et al*., 2023, Green *et al*., 2012) quite a long experiment in a small well. This could have led to overcrowding of the well resulting in the cell death. Allen *et al*., did perform an 24h assay but they used 25.000 cells which is a tenfold smaller than the number of starting cells used in this experiment (Allen, *et al*., 2016). Our experiment was performed over these 24h to be able to compare the chemokine migration with the nerve migration. It might be wise to start with a smaller number of cells in a next experiment.

The WTM2 blank was the only control almost without any moving macrophages. The migration of macrophages towards the bottom well without chemokines could be explained by gravity. They migrate towards the bottom over the duration of the experiment which was 24h. Another possibility could be that the macrophages did migrate since there was M-CSF used in all media. It would be interesting to compare migration of macrophages towards plain cell media and media containing M-CSF.

MCP1/CCL2 or monocyte attractant protein-1 is a chemokine known to attract macrophages. It plays an important role in the migration and infiltration of monocytes (Deshmane *et al*., 2009). M1 and M2c polarized macrophages can produce MCP1 (Strizova, *et al*., 2023). The results (figure 6B) show a high number of to MCP1 migrated cells for WT and CKO M1. The migration of WT and CKO M1 macrophages was almost twice as high compared to the migration of WT and CKO M2. There was more migration of CKO M0 and M1 cells compared to WT M0 and M1. M2 polarized macrophages were similar between the two genotypes. Although M2c macrophages produce MCP1, they are not activated by IL4, which is how we polarized M0 macrophages towards M2 (Strizova, *et al*., 2023). Making it unlikely that this subgroup was present in the samples.

Migration towards CST was slightly elevated in M1 macrophages of both genotypes though it was higher in WT than CKO suggesting CX_3CR1 is important for macrophage migration towards CST. Muntjewerff *et al*., found that CST blocks macrophage migration towards CCL2, CXCL2 and IL8 as well as a reduced migration of CX_3CR1+ macrophages towards CST. (Muntjewerff, at al., 2022). Our contrasting findings might stem from differences in cell types. While we employed mouse macrophages derived from bone marrow, other studies investigated the migration of both mouse and human monocytes, as well as human monocyte-derived macrophages. Additionally, our use of isolated macrophage cultures differs from research examining macrophage phenotype switching during CST treatment in specific organs (Muntjewerff, *et al*., 2022, Ying, *et al*., 2021). Moreover, the higher migration rate of macrophages in our wild-type sample could potentially be an outlier. However, since only two samples were utilized, it is not feasible to definitively identify which time point might be considered an outlier based solely on these results. CST reduces inflammation via macrophages (Briolat, *et al*., 2005) and can also initiate a phenotype change in macrophages of M1 to a more M2 like phenotype (Ying, *et al*., 2021). The phenotype of the in this experiment migrated macrophages is unknown after the first polarization. PCR is needed to compare and identify possible changes in macrophage phenotype before and after migration.

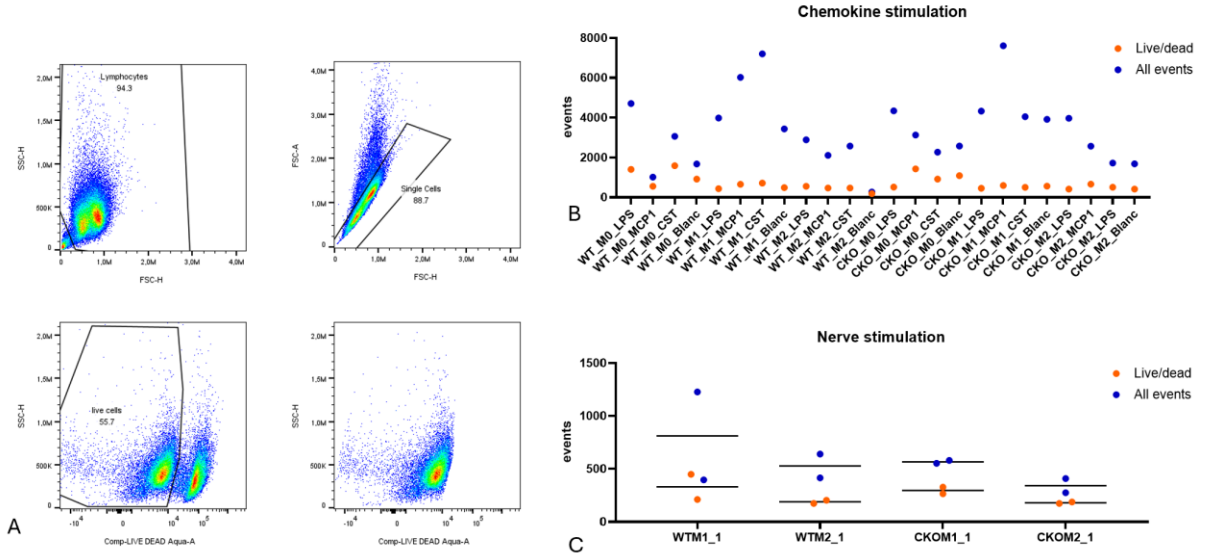

Figure 6: Migration of macrophages towards different chemokines or nerves. In this experiment, the data was gated for total cells → single cells → live cells. A single cell gate was used to separate out all the cells that stick together. A: used gaiting. B: On the x-axis, WT and CX_3CR1 KO macrophages attracted by different cytokines (LPS, MCP1 or CST). Y-axis shows the number of recorded events, live cells in orange and all single cells in blue. N=1 C: WT and CX_3CR1 KO macrophages attracted by nerves on the x-axis and the number of recorded events on the y-axis. N=2

In this experiment, the migration of CX_3CR1 KO macrophages towards nerves was compared to the WT genotype. We expected a lower migration rate of the CKO macrophages towards the nerves compared to WT macrophages since nerves produce FKN, the ligand for CX_3CR1. Without the CX_3CR1 receptor macrophages are probably unable to recognize and thus act on FKN.

Figure 6C shows the migration of macrophages towards nerves. Based on these results, CX_3CR1 KO seems to have no influence on the macrophage migration but there is a slight elevation in migration towards nerves to be observed in M1 compared to M2 polarized macrophages. Based on these preliminary results, it could be suggested that the fractalkine receptor did not influence the migration of macrophages towards nerves. This statement would be very interesting since this receptor is one of the markers for NAMs.

The total number of cells added to each well were $3x10^5$ and $2.5x10^5$ in the cytokine stimulation experiment. When comparing the experiments it was observed that less cells migrated through the filter in the nerve stimulation experiment. Additionally, a smaller number of cells died in the nerve stimulation experiment compared to the cytokine stimulation. This last observation was very interesting since the incubation time (24h) stayed the same over the two experiments. However, it can probably be explained by the lack of migrated cells, giving the cells that did migrate more space and supplements to grow. Another explanation could be that nerves are known to produce macrophage colony stimulating factor (MCSF or CSF1) which increases the proliferation of the existing population. The nerves start to produce MCSF when they notice a loss of macrophage numbers (Guilliams, *et al.*, 2020).

3.4 Fractalkine stimulation

Bone marrow derived M1 and M2 macrophages were stimulated with different concentrations of FKN to measure its influence on gene expression. Genes tested for in this experiment were IL6, iNOS and TNFa as markers for the M1 phenotype and MMR, IL10, Arg1 and Adra1 as M2 markers and GAPDH as housekeeping gene. The results of IL10 and iNOS are not shown. These primers did not work properly, and new sets should be ordered. The PCR results were quite irregular as can be seen in figure 7. One

possible reason for this could be the absence of an M0 macrophage group in this experiment, leading to the normalization of results using WT macrophage data. M1 WT was used to normalize M1 CKO, and M2 WT was used to normalize M2 CKO. This data cannot be used to draw any conclusions about the influence of different FKN concentrations on gene expression.

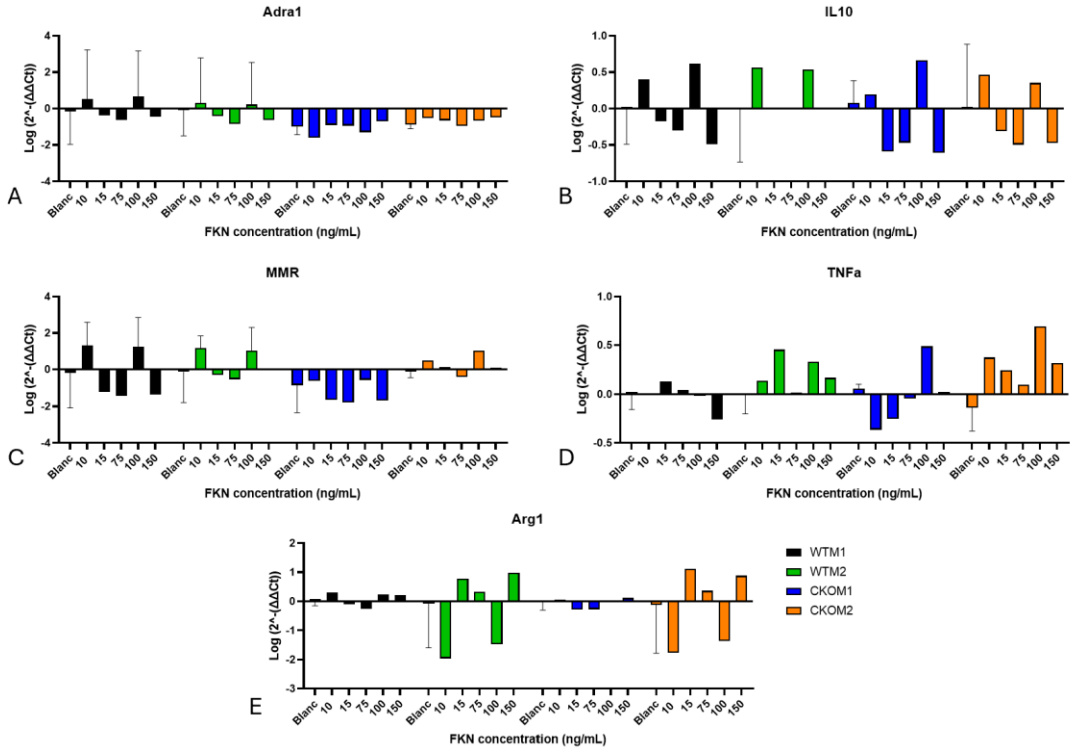

Figure 7: The influence of FKN stimulation on gene expression in M1 and M2 macrophages of WT and CX_3CR1 KO mice. Log of 2^-(ΔΔCt) on the y-axis and used FKN concentrations on the x-axis in ng/mL. WTM1 in black, WTM2 in green, CKOM1 in blue and CKOM2 in orange. A: Adra1. B: M2 marker IL10. C: M2 marker MMR. D: M1 marker TNFa and E: M2 marker Arg1. Statistics: outliers were excluded and analyzed with 2-way ANOVA, significant difference: $p < 0.05$.

When repeating this experiment there should be an M0 control group for each genotype to normalize the data across experiments. It might also be interesting to not only look at a difference in concentration but also at a difference in exposure time of macrophages to FKN. Normalizing each group with its blank did not make a difference in the results.

Following this experiment, a new experiment was conducted to look at the potential difference between macrophages of homozygote WT (WT/WT), heterozygote WT/CX_3CR1 KO (WT/CKO) and homozygote CX_3CR1 KO (CKO/CKO) mice was tested for as well as the influence of duration (6h, 8h and 12h) of macrophage polarization on gene expression.

3.5 Pro-inflammatory and anti-inflammatory gene expression in macrophages changes over time

M1 polarized macrophages were found to have an upregulation of IL6, TNFa, iNOS, IFNg and F480 while M2 polarized macrophages had an upregulation of MMR, Adra1, Adrb1, Mgl1 and Mgl2 (table 2). M0 WT/WT macrophages were used to normalize the data as well as GAPDH as a housekeeping gene. IL10 was also measured, however this primer did not work properly and should be repeated with a new primer set.

Table 2: Summary of qPCR results. Green shows an upregulation of the gene in macrophages with either M1 or M2 phenotype.

	M0	M1	M2
MMR			
IL6			
Arg1			
Adra1			
Adrb2			
TNFa			
iNOS			
IFNg			
IL4			
F480			
Mgl1			
Mgl2			

Figure 8A shows the expression of F480 represented as the log of 2^-(ΔΔCt). The results of this experiment were normalized using the WT M0 results, setting the F480 expression in WT M0 macrophages as the baseline (0) on the graphs. This normalization was performed separately for each timepoint. Values above 0 indicate higher gene expression compared to WT M0 macrophages, while values below 0 indicate lower expression. Therefore, if a bar extends below zero, it signifies that the expression was lower than that of WT M0 macrophages. The Ct obtained from the PCR are shown in figure 8B. These data were only normalized using GAPDH as housekeeping gene. The higher the bar in figure 8B, the lower the gene expression was since the Ct represents the number of PCR cycle needed to proceed the threshold. F480 is a universal macrophage marker and would be expected to be expressed in all genotypes and phenotypes.

All macrophage phenotypes with the CKOCKO genotype showed lower expression of F480. The differences between the various timepoints were minimal. Interestingly, F480 gene expression was highest in WTWT, lowest in CKOCKO, with WTCKO falling in between (figure 8).

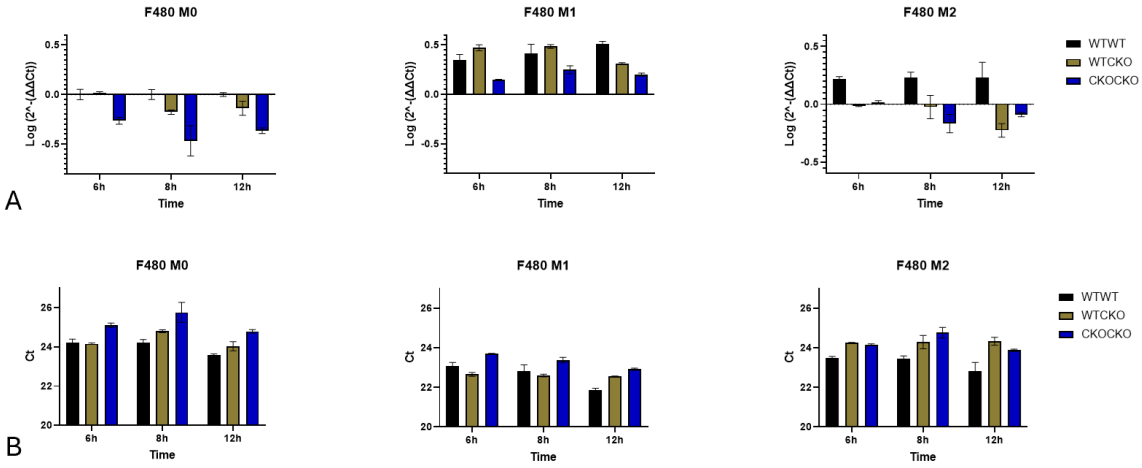

Figure 8: F480 gene expression in M0 (left), M1 (middle) and M2 (right) macrophages with three different genotypes (WT/WT, WT/CKO and CKO/CKO). Time on the x-axis. A: F480 gene expression as a Log of 2^-(ΔΔCt) on the y-axis. B: F480 gene expression as Ct on the Y-axis. Ct was normalized using GAPDH as a housekeeping gene. WTWT in black, WTCKO in brown, CKOCKO in blue. Statistics: outliers were excluded and analyzed with 2-way ANOVA, significant difference: $p < 0.05$.

M1 macrophage activation is induced by LPS and IFNg. An elevation of IFNg was found in WT/WT M1 macrophages 6 and 8h after induction of polarization (figure 9A). At 12h the gene expression went down and got similar to the other genotypes. This could be explained since polarization towards M1 is partly induced by IFNg. Once the macrophages have polarized IFNg expression might not be needed at the same levels causing it to get downregulated.

Pro-inflammatory cytokines IL6 (figure 9B) and TNFa (figure 9C) showed the highest upregulation in M1 polarized macrophages 8h after stimulation across all three genotypes. At 6 and 12h of stimulation, TNFa levels in WT/CKO were comparable to those in WT/WT M0 macrophages, and this similarity was also observed at 12h in CKO/CKO. These results could suggest that the CKO mutation influences long term TNFa expression.

The iNOS expression in M1 macrophages was in general upregulated compared to M0 and M2 (figure 9D). M1 polarized WT/CKO macrophages had a lower iNOS gene expression 6h after polarization compared to WT/WT and CKO/CKO macrophages. This was interesting since there was an upregulated expression in M0 WT/CKO at the 6h point which was not observed in the other two genotypes. The expression of iNOS went down in WT/CKO and CKO/CKO M1 macrophages 12h after polarization.

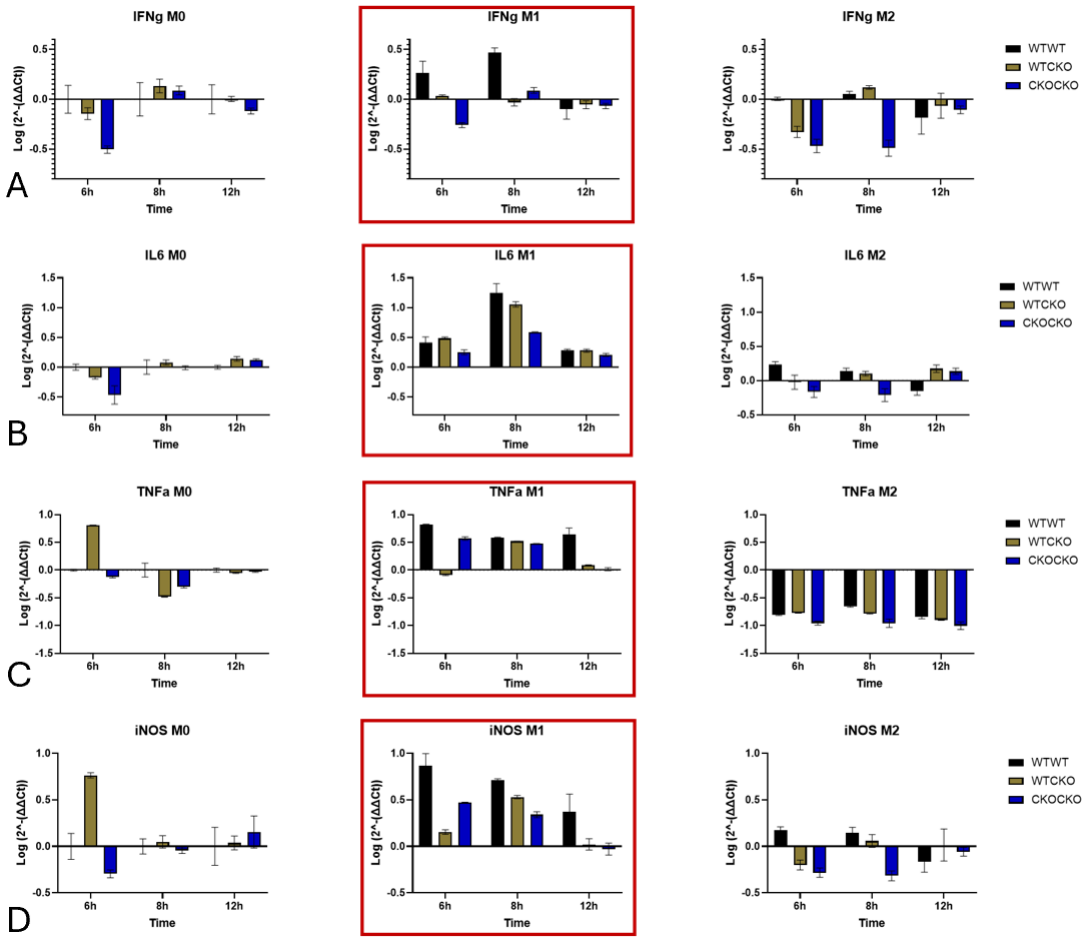

Figure 9: Gene expression of M1 markers with M0 macrophages as a control. A – D: M1 (middle) and M2 (right) macrophages with three different genotypes (WT/WT, WT/CKO and CKO/CKO). Log of 2^-(ΔΔCt) on the y-axis and time on the x-axis. WTWT in black, WTCKO in brown, CKOCKO in blue. Statistics: outliers were excluded and analyzed with 2-way ANOVA, significant difference: $p < 0.05$.

Although M2 macrophages are typically induced by IL4, this experiment did not demonstrate any clear upregulation in macrophages with the M2 phenotype or any of the other tested phenotypes (figure 10A). Since the results did not match expectations, the primer sequence was blasted against the Mus musculus genome, revealing a product of IL4. However, there was a mismatch in the primer sequence with the target gene, which could explain the irregular data. The experiment should be repeated with a new primer set to measure IL4 expression in WT/WT, WT/CKO, and CKO/CKO M1 and M2 macrophages at the 6h, 8h, and 12h time points.

Two other M2 macrophage markers, MMR (figure 10B) and Arg1 (figure 10C), showed an upregulation for all genotypes in M2 stimulated macrophages. MMR showed an upregulation at each measured time point and for all genotypes in M2 stimulated macrophages. While Arg1 only showed an upregulation 8 and 12h after polarization. Arg1 production in macrophages is activated after IL4 stimulation (Colegio, *et al*., 2014). According to these results, 6h of IL4 stimulation is not enough time to cause an upregulation in Arg1 production.

Expression of adrenergic receptors (ADR) by immune cells is needed to release anti-inflammatory sympathetic neurotransmitters. These ADR can be separated into two groups, Adra and Adrb, which can also each be divided into subgroups. In this study, we focused on Adra1 and Adrb2. Adra1 stimulation triggers pro-inflammatory immune responses, whereas Adrb2 stimulation activates anti-inflammatory immune responses (Ribeiro da silva., *et al*., 2018). Adra1 results showed elevated expression levels at 6 hours in M2 polarized macrophages for all three genotypes (figure 10D). This expression decreased to levels similar to those in M0 and M1 macrophages by the 8h mark and remained constant after 12h of stimulation. Adrb2 also had a higher gene expression for M2 macrophages 6h after stimulation (figure 10E). Interestingly, this elevation was only found in macrophages with the WT/WT and WT/CKO phenotype. This would suggest that CX_3CR1 is needed for nerve-macrophage interactions. The Adrb2 levels went down after time passed with its lowest point 12h after stimulation. This might have happened because of an absence of nerves in this cell culture, making the secretion of neurotransmitters unnecessary.

The data for both Adra1 and Adrb2 are not really giving a clear view on gene expression. This could be since there were no nerves present in the cell culture and since these receptors are activated by neurotransmitters (Freire, *et al*., 2022), it would make sense for the macrophages to not waste energy on gene expression when there are no neurotransmitters present. This hypothesis could be tested by coculturing M1 or M2 stimulated macrophages with nerves during different time points after which the macrophage mRNA can be isolated for qPCR.

Mgl1 and Mgl2 are genes specific to macrophages with a M2 phenotype. These genes negatively influence cell migration and effector T cell function (Westcott, *et al*., 2009). The results showed an upregulation of Mgl1 (figure 10F) and Mgl2 (figure 10G) in M2 stimulated macrophages for all three genotypes. Mgl1 expression in WT/CKO M2 macrophages went down over time but stayed the same in Mgl2. CKO/CKO had the lowest expression over all three timepoints for Mgl2 as wel as Mgl1 after 6 and 8h of polarization.

These results show the importance of the duration of polarization of macrophages on gene expression. There were also slight differences found in between the three different genotypes. A lot of PCR samples were used in this experiment, however the cell culture is only done once. The experiment should be repeated to compare the results.

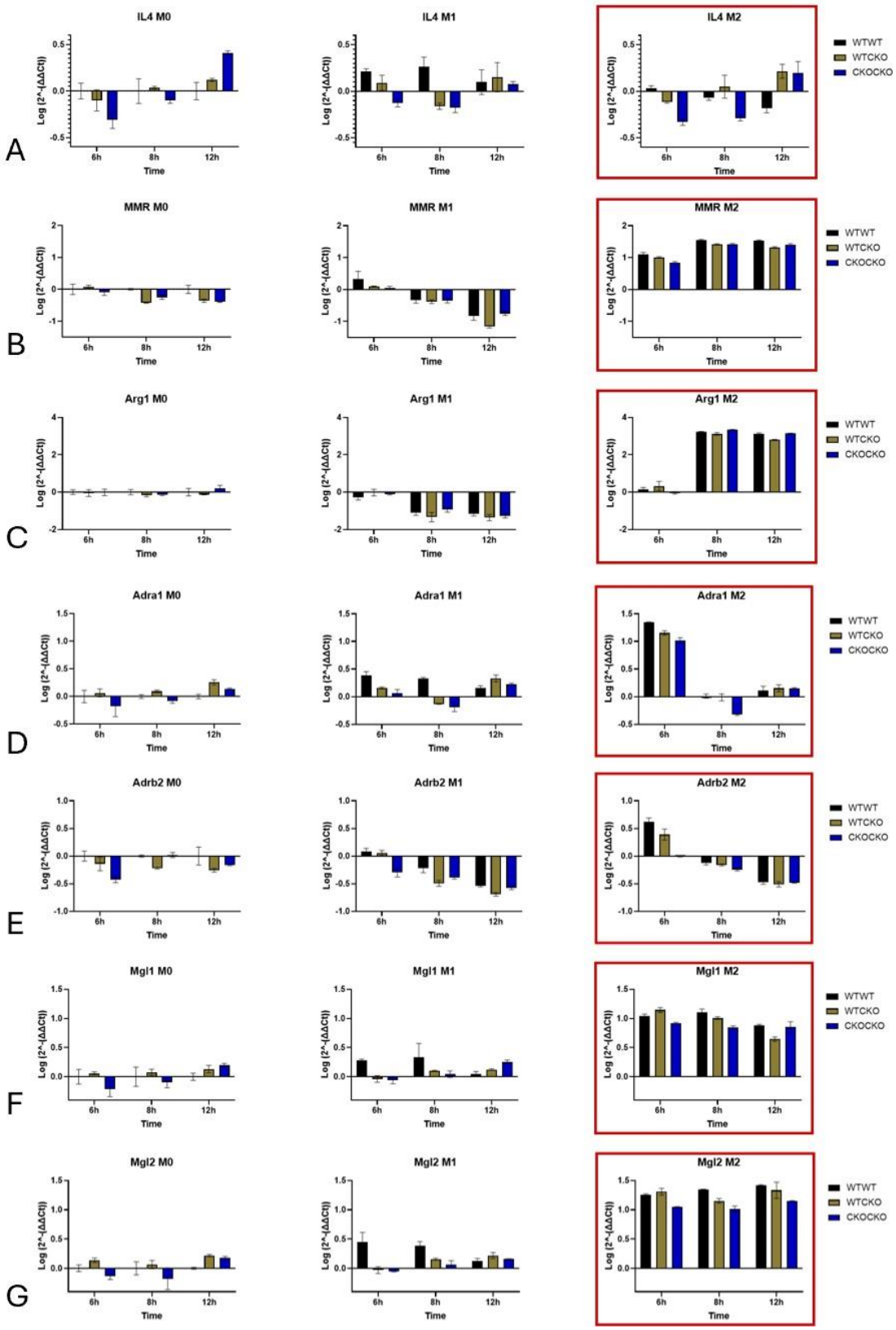

Figure 10: Gene expression of M2 markers. A – G: M1 (middle) and M2 (right) macrophages with three different genotypes (WT/WT, WT/CKO and CKO/CKO). Log of 2^-(ΔΔCt) on the y-axis and time on the x-axis. WTWT in black, WTCKO in brown, CKOCKO in blue. Statistics: outliers were excluded and analyzed with 2-way ANOVA, significant difference: $p < 0.05$.

References

Ahren, B. (2000). Autonomic regulation of islet hormone secretion—implications for health and disease. *Diabetologia*, 43: 393-410.

Allen, S. G., Chen, Y.-C., Madden, J. M., Fournier, C. L., Altemus, M. A., Hiziroglu, A. B., . . . Merajver, S. D. (2016). Macrophages Enhance Migration in Inflammatory Breast Cancer Cells via RhoC GTPase Signaling. *Scientific reports*, 39190.

Aoyama, T., Inokuchi, S., Brenner, D. A., & Seki, E. (2010). CX3CL1-CX3CR1 interaction prevents CCl4-induced liver inflammation and fibrosis. *Hepatology*, 52(4): 1390-1400.

Baker, R. L., Bradley, B., Wiles, T. A., Lindsay, R. S., Barbour, G., Delong, T., . . . Haskins, K. (2016). Cutting Edge: Nonobese Diabetic Mice Deficient in Chromogranin A Are Protected from Autoimmune Diabetes. *J. Immunol.*, 196(1): 39-43.

Banek, C. T., Gauthier, M. M., Van Helden, D. A., Fink, G. D., & Osborn, J. W. (2019). Renal Inflammation in DOCA-Salt Hypertension: Role of Renal Nerves and Arterial Pressure. *Hypertension*, 73: 1079-1086.

Bartolomucci, A., Possenti, R., Mahata, S. K., Fischer-Colbrie, R., Loh, Y., & Salton, S. R. (2011). The extended granin family: structure, function, and biomedical implications. *Endocr. rev.*, 32(6):755-797.

Bockman, D. E. (2007). Nerves in the pancreas: what are they for? *The American Journal of Surgery*, 194 (4): S61-S64.

Böni-Schnetzler, M., & Meier, D. T. (2019). Islet inflammation in type 2 diabetes. *Seminars in immunopathology*, 501–513.

Borovikova, L. V., Ivanova, S., Zhang, M., Yang, H., Botchkina, G. I., Watkins, L. R., . . . Tracey, K. J. (2000). Vagus nerve stimulation attenuates the systemic inflammatory response to endotoxin. *Nature*, 405(6785):458-62.

Bralewska, M., Pietrucha, T., & Sakowicz, A. (2024). The Role of Catestatin in Preeclampsia. *Int. J. Mol. Sci.*, 25(5): 2461.

Calderon, B., Carrero, J. A., Ferris, S. T., Sojka, D. K., Moore, L., Epelman, S., . . . Unanue, E. R. (2015). The pancreas anatomy conditions the origin and properties of resident macrophages. *Journal of Experimental Medicine*, 212(10): 1497-1512.

Campbell-Thompson, M., Butterworth, E. A., Boatwright, J. L., Nair, M. A., Nasif, L. H., Revell, A. Y., . . . Atkinson, M. A. (2021). Islet sypmathetic innervation and islet neuropathology in patients with type 1 diabetes. *Scientific reports*, 11:6562.

Cardona, A. E., Pioro, E. P., Sasse, M. E., Kostenko, V., Cardona, S. M., Dijkstra, I. M., . . . Ransohoff, R. M. (2006). Control of microglial neurotoxicity by the fractalkine receptor. *Nat. Neurosci*, 9(7): 917-24.

Chen, H., Liu, N., & Zhuang, S. (2022). Macrophages in Renal Injury, Repair, Fibrosis Following Acute Kidney Injury and Targeted Therapy. *Front. Immunol.*, volume 13.

Chiao, Y., Dai, Q., Zhang, J., Lin, J., Lopez, E. F., Ahuja, S. S., . . . Jin, Y.-F. (2011). Multi-Analyte Profiling Reveals Matrix Metalloproteinase-9 and Monocyte Chemotactic Protein-1 as Plasma Biomarkers of Cardiac Aging. *Genomic and Precision Medicine*, 4: 455-462.

Christoffersson, G., Ratliff, S. S., & Von Herrath, M. G. (2020). Interference with pancreatic sympathetic signaling halts the onset of diabetes in mice. *Science advances*, Vol. 6, NO. 35 .

Colegio, O. R., Chu, N.-Q., Szabo, A. L., Chu, T., Rhebergen, A., Jairam, V., . . . Medzhitov, R. (2014). Functional polarization of tumour-associated macrophages by tumour-derived lactic acid. *Nature*, 513(7519): 559-563.

Coppieters, K. T., Dotta, F., Amirian, N., Campbell, P. D., Kay, T. W., Atkinson, M. A., . . . von Herrath, M. G. (2012). Demonstration of islet-autoreactive CD8 T cells in insulitic lesions from recent onset and long-term type 1 diabetes patients. *Journal of experimental medicine*, 209(1): 51-60.

Dadfar, E., Ghaderi, A., Moshfegh, A., Barcenilla, H., Casas, R., & Samuelsson, U. (2020). Reduced level of CX3CR1 positive T-cells and monocytes in children with, newly diagnosed, Type 1 diabetes. *The journal of immunology*, 204 (1_Supplement): 59.7.

Davies, L. C., Jenkins, S. J., Allen, J. E., & Taylor, P. R. (2014). Tissue-resident macrophages. *Nat Immunol.*, 14(10): 986-995.

De Schepper, S., Verheijden, S., Aguilera-Lizarraga, J., Viola, M., Boesmans, W., Stakenborg, N., . . . *et al*. (2018). Self-maintaining gut macrophages are essential for intestinal homeostasis. *Cell*, 175: 400-415.

Deshmane, S. L., Kremlev, S., Amini, S., & Sawaya, B. E. (2009). Monocyte Chemoattractant Protein-1 (MCP-1): An Overview. *J. Interferon Cytokine Res*, 29(6): 313-326.

DiMeglio, L. A., Evans-Molina, C., & Oram, R. A. (2018). Type 1 Diabetes. *Lancet*, 16;391(10138):2449-2462.

Freire, B. M., Menegatti de Melo, F., & Basso, A. S. (2022). Adrenergic signaling regulation of macrophage function: do we understand it yet? *Immunotherapy Advances*, Volume 2 issue 1.

Gauthier, M. M., Hayoz, S., & Banek, C. T. (2023). Neuroimmune interplay in kidney health and disease: Role of renal nerves. *Autonomic Neuroscience*, 250: 103133.

Green, T. D., Park, J., Yin, Q., Fang, S., Crews, A. L., Jones, S. L., & Adler, K. B. (2012). Directed migration of mouse macrophages in vitro involves myristoylated alanine-rich C-kinase substrate (MARCKS) protein. *Journal of Leukocyte Biology*, 92(3): 633-639.

Gregg, B., Lumeng, C. N., & Bernal-Mizrachi, E. (2014). Fractalkine signaling in regulation of insulin secretion: Mechanisms and potential therapeutic implications? *Islets*, 6(1).

Guilliams, M., Thierry, G. R., & Bonnardel, J. (2020). Establishment and maintenance of the Macrophage Niche. *Immunity*, 52(3): 434-451.

Hasegawa, S., Inoue, T., & Inagi, R. (2019). Neuroimmune interactions and kidney disease. *Kidney Res. Clin. Pract*, 38(3): 282-294.

Hull, C. M., Peakman, M., & Tree, T. I. (2017). Regulatory T cells dysfunction in type 1 diabetes: what's broken and how can we fix it? *Diabetologia*, 60(10): 1839-1850.

Imai, T., Hieshima, K., Haskell, C., Baba, M., Nagira, M., Nishimura, M., . . . Yoshie, O. (1997). Identification and molecular characterization of fractalkine receptor CX3CR1, which mediates both leukocyte migration and adhesion. *Cell*, 91(4):521-30.

Justus, C. R., Marie, M. A., Sanderlin, E. J., & Yang, L. V. (2023). Transwell In Vitro Cell Migration and Invasion Assays. *Methods in molecular biology*, 349.359.

Kolter, J., Kierdorf, K., & Hanneke, P. (2020). Origin and Differentiation of Nerve-Associated Macrophages. *The journal of immunology*, 204(2):271-279.

Liu, F., Dai, S., Feng, D., Qin, Z., Peng, X., Sakamuri, S. S., . . . Qin, X. (2020). Distinct fate, dynamics and niches of renal macrophages of bone marrow or embryonic origins. *Nature Communications*, 2280.

Ma, Y., Mouton, A. J., & Lindsey, M. L. (2018). Cardiac macrophage biology in the steady-state heart, the aging heart, and following myocardial infarction. *Translational Research*, 191: 15-28.

Mahapatra, N. R. (2008). Catestatin is a novel endogenous peptide that regulates cardiac function and blood pressure. *Cardiovascular Research*, 80(3): 330-338.

Mahapatra, N. R., O'Connor, D. T., Vaingankar, S. M., Sinha Hikim, A. P., Mahata, M., Ray, S., . . . Mahata, S. K. (115(7): 1942-52). Hypertension from targeted ablation of chromogranin A can be rescued by the human ortholog. *2005*.

McWhorter, F. Y., Davis, C. T., & Liu, W. F. (2015). Physical and mechanical regulation of macrophage phenotype and function. *Cell. Mol. Life Sci.*, 72(7) 1303-1316.

Mills, C. D., Kincaid, K., Alt, J. M., Heilman, M. J., & Hill, A. M. (2000). M-1/M-2 macrophages and the Th1/Th2 paradigm. *The journal of immunology*, 6166–6173.

Mundinger, T. O., Mei, Q., Foulis, A. K., Fligner, C. L., Hull, R. L., & Taborsky Jr, G. J. (2016). Human Type 1 Diabetes Is Characterized by an Early, Marked, Sustained, and Islet-Selective Loss of Sympathetic Nerves. *Diabetes*, 65(8):2322-30.

Muntjewerff, E. M., Christoffersson, G., Mahata, S. K., & Bogaart van den, G. (2021). Putative regulation of macrophage-mediated inflammation by catestatin. *Opinion*, volume 43, issue 1, p41-50.

Muntjewerff, E. M., Josyula, V. S., & Christoffersson, G. (2023). Three-dimensional Co-culture Model For Live Imaging of Pancreatic Islets, Immune Cells And Neurons In Agarose Gel. *Bio_protocol*, preprint.

Muntjewerff, E. M., Parv, K., Mahata, S. K., Riessen van, N. K., Phillipson, M., Christoffersson, G., & Bogaart van den, G. (2022). The anti-inflammatory peptide Catestatin blocks chemotaxis. *J. Leukoc biol.*, 112(2): 273-278.

Ribeiro-da-Silva, M., Vasconcelos, D. M., Alencastre, I. S., Oliveira, M. J., Linhares, D., Neves, N., . . . Alves, C. J. (2018). Interplay between sympathetic nervous system and inflammation in aseptic loosening of hip joint replacement. *Scientific Reports*, 8: 16044.

Richardson, S. J., Rodriguez-Calvo, T., Gerling, I. C., Mathews, C. E., Kaddis, J. S., Russell, M. A., . . . Morgan, N. G. (2016). Islet cell hyperexpression of HLA class I antigens: a defining feature in type 1 diabetes. *Diabetologia*, 59(11): 2448-2458.

Rodriguez-Calvo, T., Suwandi, J. S., Amirian, N., Zapardiel-Gonzalo, J., Anquetil, F., Sabouri, S., & von Herrath, M. G. (2015). Heterogeneity and Lobularity of Pancreatic Pathology in Type 1 Diabetes during the Prediabetic Phase. *Journal of Histochemistry and Cytochemistry*, 63(8): 626-636.

Rodriguez-Diaz, R., & Caicedo, A. (2014). Neural control of the endocrine pancreas. *Best Practice and Research Clinical Endocrinology and Metabolism*, Volume 28, Issue 5, P745-756.

Rodriguez-Diaz, R., Abdulreda, M. H., Formoso, A. L., Gans, I., Ricordi, C., Berggren, P.-O., & Caicedo, A. (2011). Innervation Patterns of Autonomic Axons in the Human Endocrine Pancreas. *Cell metabolism*, Volume 14, Issue 1, P45-54.

Sabatel, C., Radermecker, C., Fievez, L., Paulissen, G., Chakarov, S., Fernandes, C., . . . Bureau, F. (2017). Exposure to Bacterial CpG DNA Protects from Airway Allergic Inflammation by Expanding Regulatory Lung Interstitial Macrophages. *Immunity*, 46(3): 457-473.

Shah, R. V., Truong, Q. A., Gaggin, H. K., Pfannkuche, J., Hartmann, O., & Januzzi Jr, J. L. (2012). Mid-regional pro-atrial natriuretic peptide and pro-adrenomedullin testing for the diagnostic and prognostic evaluation of patients with acute dyspnoea. *Eur Heart J.*, 33(17): 2197-205.

Shen, D., Chu, F., Lang, Y., Geng, Y., Zheng, X., Zhu, J., & Liu, K. (2018). Benificial or harmful role of macrophages in Guillain-Barré syndrome and experimental autoimmune neuritis. *Mediators inflamm.*, 4286364.

Sindhu, S., Akhter, N., Arefanian, H., Al-Roub, A. A., Ali, S., Wilson, A., . . . Ahmad, R. (2017). Increased circulatory levels of fractalkine (CX3CL1) are associated with inflammatory chemokines and cytokines in individuals with type-2 diabetes. *J. Diabetes. Metab. Disord.*, 16(15).

Steinman, L. (2004). Elaborate interactions between the immune and nervous systems. *Nature immunology*, 575-581.

Strizova, Z., Benesova, I., Bartolini, R., Novysedlak, R., Cecrdlova, E., Foley, L. K., & Striz, I. (2023). M1/M2 macrophages and their overlaps – myth or reality? *Clinical science*, 137(15): 1067-1093.

Tatemoto, K., Efendić , S., Mutt, V., Makk, G., Feistner, G. J., & Barchas, J. D. (1986). Pancreastatin, a novel pancreatic peptide that inhibits insulin secretion. *Nature*, 324(6096): 476-478.

Tsubota, K., Nishiyama, T., Mishima, K., Inoue, H., Doi, T., Hattori, Y., . . . Saito, I. (2009). The role of fractalkine as an accelerating factor on the autoimmune exocrinopathy in mice. *Invest. Ophthalmol. Vis. Sci*, 50(10): 4753-60.

Ural, B. B., Yeung, S. T., Sawai, C. M., Jang, G., Perez, O. A., Pham, Q., . . . Khanna, K. M. (2020). Identification of a nerve-associated, lung-resident interstitial macrophage subset with distinct localization and immunoregulatory properties. *Sci Immunol*, 5(45): eaax8756.

Velthuis, J. H., Unger, W. W., Abreu, J. R., Duinkerken, G., Franken, K., Peakman, M., . . . Roep, B. O. (2010). Simultaneous Detection of Circulating Autoreactive CD8+ T-Cells Specific for Different Islet Cell–Associated Epitopes Using Combinatorial MHC Multimers. *Diabetes*, 59(7): 1721-1730.

Westcott, D. J., DelProposto, J. B., Geletka, L. M., Singer, K., Saltiel, A. R., & Lumeng, C. N. (2009). MGL1 promotes adipose tissue inflammation and insulin resistance by regulating 7/4hi monocytes in obesity. *Journal of Experimental Medicine*, 206(13): 3143-3156.

Ying, W., Fu, W., & Lee, Y. (2019). Role of macrophages in obesity-associated islet inflammation and beta cell abnormalities. *Nat Rev Endocrinol*, 81-90.

Ying, W., Mahata, S., Bandyopadhyay, G. K., Zhou, Z., Wollam, J., Vu, J., . . . Mahata, S. K. (2018). Catestatin Inhibits Obesity-Induced Macrophage Infiltration and Inflammation in the Liver and Suppresses Hepatic Glucose Production, Leading to Improved Insulin Sensitivity. *Diabetes*, 67(5): 841-848.

Ying, W., Tang, K., Avolio, E., Schilling, J. M., Pasqua, T., Liu, M. A., . . . Mahata, S. K. (2021). The immunosuppression of macrophages underlies the cardioprotective effects of catestatin (CST). *Hypertension*, 77(5): 1670-1682.

Zaynagetdinov, R., Sherrill, T. P., Kendall, P. L., Segal, B. H., Weller, K. P., Tighe, R. M., & Blackwell, T. S. (2013). Identification of Myeloid Cell Subsets in Murine Lungs Using Flow Cytometry. *Am J Respir Cell Mol Biol.*, 49(2): 180–189.

Zheng, X.-F., Hong, Y.-X., Feng, G.-J., Zhang, G.-F., Rogers, H., Lewis, M. A., . . . Wei, X.-Q. (2013). Lipopolysaccharide-Induced M2 to M1 Macrophage Transformation for IL-12p70 Production Is Blocked by Candida albicans Mediated Up-Regulation of EBI3 Expression. *Plos One*, 8(5): e63967.

Zhu, Q., Xiao, L., Cheng, G., He, J., Yin, C., Wang, L., . . . Shi, P. (2023). Self-maintaining macrophages within the kidney contribute to salt and water balance by modulating kidney sympathetic nerve activity. *Kidney International*, 104(2): 324-333.

Supplementary data

I. Heart innervation and colocalization/nerve volume